

Journal of Biomedical Optics

SPIEDigitalLibrary.org/jbo

Method to calibrate phase fluctuation in polarization-sensitive swept-source optical coherence tomography

Zenghai Lu
Deepa K. Kasaragod
Stephen J. Matcher



Method to calibrate phase fluctuation in polarization-sensitive swept-source optical coherence tomography

Zenghai Lu, Deepa K. Kasaragod, and Stephen J. Matcher

University of Sheffield, The Kroto Institute, Department of Materials Science and Engineering, North Campus, Broad Lane, Sheffield, S3 7HQ, United Kingdom

Abstract. We present a phase fluctuation calibration method for polarization-sensitive swept-source optical coherence tomography (PS-SS-OCT) using continuous polarization modulation. The method uses a low-voltage broadband polarization modulator driven by a synchronized sinusoidal burst waveform rather than an asynchronous waveform, together with the removal of the global phases of the measured Jones matrices by the use of matrix normalization. This makes it possible to average the measured Jones matrices to remove the artifact due to the speckle noise of the signal in the sample without introducing auxiliary optical components into the sample arm. This method was validated on measurements of an equine tendon sample by the PS-SS-OCT system. ©2011 Society of Photo-Optical Instrumentation Engineers (SPIE). [DOI: 10.1117/1.3597721]

Keywords: phase fluctuation; polarization-sensitive swept-source optical coherence tomography; broadband polarization modulator; triggered tone-burst mode; matrix normalization.

Paper 11150LR received Mar. 25, 2011; revised manuscript received May 17, 2011; accepted for publication May 17, 2011; published online Jul. 18, 2011.

1 Introduction

Polarization-sensitive optical coherence tomography (PS-OCT) can nondestructively determine the optical birefringence of turbid materials such as biological tissue in a depth-resolved manner.¹ Recently, a fiber-based swept-source PS-OCT (PS-SS-OCT) has been reported.² However, the system phase fluctuation results in an artifact of the measurement since the PS-SS-OCT is a phase-sensitive system. The sources of the phase fluctuation are i. the jitter between the start trigger of the wavelength sweeping generated by the light source (which is typically called the “A-scan trigger”) and the rising edge of the analog-to-digital converter (ADC) sampling clock, and ii. the asynchronous driving between the ADC sampling clock and the polarization modulation introduced by the electro-optic modulator (EOM). A necessary step in PS-OCT is to measure the Jones matrix of the surface Fresnel reflection from a sample³ and for optimum accuracy, one usually would like to average this

across a number of A-scans. However, these phase fluctuations preclude direct averaging. A previous report⁴ applied averaging for the measured Jones matrices after compensating these phase fluctuations by introducing one or more static reference reflectors into the sample arm to remove the artifact due to the speckle noise of the signal at the sample surface and in the sample.

In this Letter, we remove the effect of the phase fluctuations on the measurement without introducing auxiliary optical components into the sample arm. This is realized by using the triggered tone-burst mode of a function generator to drive a low-voltage broadband modulator synchronously with the A-scan wavelength sweep. Matrix normalization is used in software-based postprocessing to eliminate the global phases of the measured surface Jones matrices induced by jitter between the A-scan trigger and the ADC sampling clock. Measurements on the equine tendon illustrates improvements, especially in fast-axis images, by using the method presented.

2 System and Theory

The PS-SS-OCT system used for this work has already been described in our previous paper.² Briefly, the light is polarized and then modulated continuously by an EOM (PC-B3-00-SFAP-SFA-130, EOSpace) operating at 6.7 MHz. The EOM can be driven from dc up to tens of Megahertz, and the limit is due to the required drive voltages which lead to large slew rates at a high frequency. More importantly, this device is a waveguide modulator rather than a crystal modulator, hence, it possesses a broadband frequency response even with low voltage drive waveforms of 20 V or less. In comparison, broadband crystal modulators require drive voltages of several hundred volts. Low-voltage crystal modulators exist, however, these are resonant devices which employ a high-Q resonant tank circuit to boost the low-voltage drive signal and thus, only work at a specific harmonic frequency. It is then extremely difficult to drive these synchronously with an external timing signal. The modulated light is split into the reference and sample arm, recombined, and detected. The theoretical description and data processing procedures of the system have been previously described.^{2,5} The depth-resolved Jones matrices algebraically calculated from the experimental data can be described as,²

$$J''_{\text{measured}} = e^{i2\alpha z \varepsilon(n)} J_{\text{out}} J_{\text{sample}} J_{\text{in}} J_{\text{offset2}}, \quad (1)$$

where α is the wavenumber-sweeping rate of the light source ($-8.1 \times 10^9 \text{ m}^{-1} \text{ s}^{-1}$), $\varepsilon(n)$ is the acquisition timing offset of the n 'th A-scan, J_{sample} is a depth-dependent double-pass Jones matrix of the sample, J_{in} and J_{out} are Jones matrices representing birefringence of the system fiber-optic components, and J_{offset2} is a unitary matrix induced by the phase offset between the polarization modulation and the A-scan trigger and is characterized as

$$J_{\text{offset2}} = 0.5 \begin{pmatrix} e^{-i\delta(n)} + 1 & e^{-i\delta(n)} - 1 \\ e^{-i\delta(n)} - 1 & e^{-i\delta(n)} + 1 \end{pmatrix}, \quad (2)$$

where $\delta(n)$ is the phase offset of the n 'th A-scan caused by the asynchronous driving between the ADC sampling clock and the EOM. To compensate the fiber-induced birefringence in the sample arm fiber, the Jones matrix at the sample surface is used as a reference matrix to calculate the birefringence in the sample.

Address all correspondence to: Zenghai Lu, University of Sheffield, Broad Lane, Sheffield, South Yorkshire S3 7HQ, United Kingdom. Tel: 44 114 2225994; E-mail: z.lu@sheffield.ac.uk.

The Jones matrix at the sample surface can be expressed as

$$J''_{\text{surface}} = e^{i2\alpha z \varepsilon(n)} J_{\text{out}} J_{\text{in}} J_{\text{offset2}}. \quad (3)$$

We can only measure J''_{surface} and depth-resolved J''_{measured} . To obtain the phase retardance η and fast-axis orientation θ of the sample, matrix diagonalization is applied to the following equation,

$$\begin{aligned} J_{c,m} &= J''_{\text{measured}} J_{\text{surface}}^{-1} = J_{\text{out}} J_{\text{sample}} J_{\text{out}}^{-1} \\ &= J_U \begin{pmatrix} p_1 e^{i\eta/2} & 0 \\ 0 & p_2 e^{-i\eta/2} \end{pmatrix} J_U^{-1}, \end{aligned} \quad (4)$$

where p_1, p_2 are two transmittances of the eigenvectors of the sample, and J_U is a general unitary matrix, whose columns are the fast and slow eigenpolarizations of $J_{c,m}$. θ is extracted from these eigenpolarizations. The degree of the phase retardance can be extracted through the phase difference of the resulting diagonal elements.

However, in measurements made on biological tissue such as equine tendon, the extracted J''_{surface} from each A-scan can be distorted due to the speckle noise of the signal at the sample surface. This can degrade the calculated birefringence images. Averaging for the surface signals can be applied to reduce the artifact,² however, it is not possible due to the system phase fluctuations. Therefore, they should be calibrated first.

The light source has a polygon mirror scanner and cannot be synchronized to an external source, however, the broadband EOM used is driven by an arbitrary waveform function generator (33120A, Agilent) and an RF amplifier (BTM00250, Tomco). The use of an arbitrary waveform generator allows the EOM to be synchronized to the light source k -sweep using an externally triggered sinusoidal tone burst, which then completely removes J_{offset2} in Eqs. (1) and (3) from each A-scan. The number of generated sinusoidal cycles should cover the duration of the A-scan sweep. The averaging of the measured surface Jones matrix J''_{surface} across A-scans is then possible provided that we remove the global phase offset term $e^{i2\alpha z \varepsilon(n)}$ from each A-scan first. Under the reasonable assumption that all the Jones matrices in Eq. (3) are unit-determinant unitary (i.e., there is negligible polarization-dependent loss in the fibers and couplers) J''_{surface} is normalized by using the matrix determinant which is expressed as

$$J'''_{\text{surface}} = \frac{J''_{\text{surface}}}{\sqrt{\det(J''_{\text{surface}})}}, \quad (5)$$

where J''_{surface} can be directly normalized to have the unit determinant since J_{in} and J_{out} can be treated as unitary matrices if the optical system represented by them is nondiattenuating.³ The global phases of J'''_{surface} are then normalized by the phases of their first column and first row elements to remove the sign ambiguity introduced in Eq. (5), because the root of determinant would decrease a range of the phase to be $\pm \pi/2$. J'''_{surface} can then be directly averaged across A-scans to provide a high accuracy estimate of $J_{\text{out}} J_{\text{in}}$.

3 Experimental Results

An example of the generated synchronized 10-cycle waveform using the A-trigger signal as an external trigger source to the triggered tone burst mode of the generator is shown in

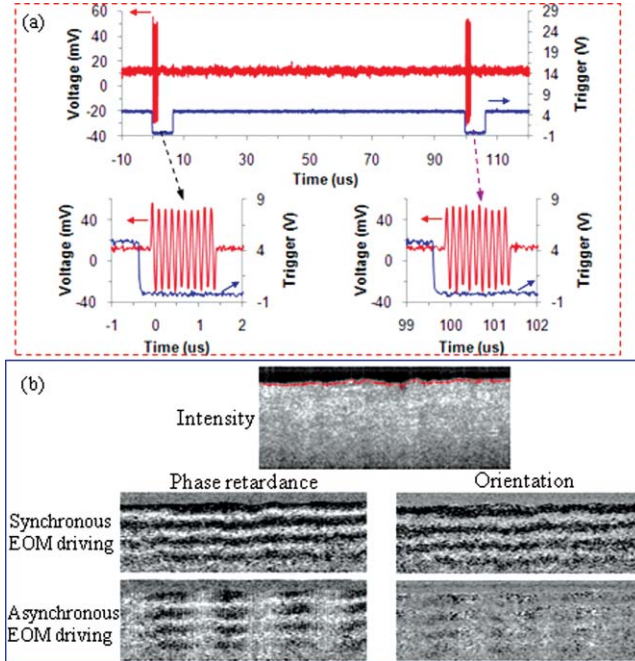


Fig. 1 (a) Example of the generated synchronized 10-cycle sinusoidal waveform using the A-trigger signal from the swept source as an external trigger source by using the triggered tone-burst mode of the function generator. (b) Measured phase retardance and orientation images on the same equine tendon sample by using asynchronous and synchronous EOM driving.

Fig. 1(a). After modest amplification, the signal is used to drive the EOM directly. It can be clearly seen that the A-trigger and the EOM are synchronized in our system for each A-scan. This was further verified by the comparison of measurements on the same equine tendon sample when asynchronous and synchronous EOM driving was implemented in the PS-SS-OCT system. Figure 1(b) shows the measured phase retardance and orientation images of the sample. Artifacts seen as blurred regions are observed in the images obtained when the asynchronous EOM driving was used. This is because the reference matrix (i.e., the averaged surface Jones matrix) is inaccurately extracted due to the existence of J_{offset2} among each A-scan. However, these artifacts were greatly reduced when the synchronous EOM driving was used, resulting from the removal of J_{offset2} among each A-scan.

An equine tendon sample was used as a test target to validate the proposed method, where 450 cycles of sine waveform were generated using the tone-burst mode to drive the EOM to cover the duty cycle of the light source. Comparison was also made between the proposed method and the other method in which the surface Jones matrix is extracted for each A-scan. We describe the latter as the direct-calibration method. The results are shown in Fig. 2. Artifacts seen as vertical white stripes are observed in the phase retardance and orientation images processed using the direct-calibration method. The artifacts result from either speckle noise of the signal at the sample surface and/or detector saturation by excessive Fresnel reflection from certain points on the sample surface. The extracted locations of the sample surface are shown as red dots in the intensity image. When the signal from the surface is degraded by the speckle noise and/or saturated, the surface Jones matrix is inaccurately

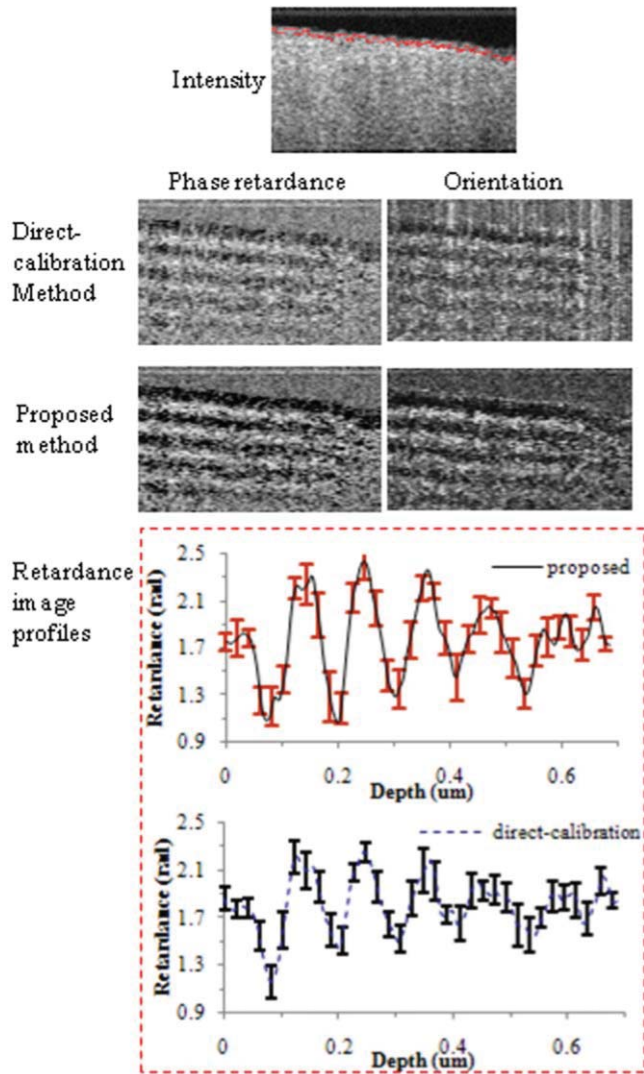


Fig. 2 Measured phase retardance and orientation images of equine tendon by using the proposed method and the direct-calibration method of determining the surface Jones matrix, respectively. Profiles of images are also included, together with the variance about the mean.

extracted, leading to an inaccurate estimate of $J_{out}J_{in}$ which reduces the success of matrix diagonalization, and thus degrades the calculated birefringence images. However, the artifacts were greatly reduced by using the proposed method. This is because the speckle noise of the signal at the sample surface is largely eliminated by averaging the measured surface Jones matrices.

Image profiles were generated by averaging the profile among A-scans to illustrate quantitatively the improvement of the proposed method over the direction-calibration method as shown in Fig. 2. The peak-to-valley measures in the phase retardance profiles close to the sample surface are 1.32 and 0.83 radians for the proposed and direction-calibration method, respectively. The variances of each phase retardance A-scan about the mean are also calculated and shown in both retardance profiles. The signal-to-noise ratio (SNR), characterized as the signal to the square root of the variance of the phase retardance, is estimated

to be 13.5 and 6.5 for the proposed and direction-calibration method, respectively. This clearly shows that the image contrast obtained by the proposed method is better than that obtained by the direct-calibration method.

4 Conclusion

The theory and experiment demonstrated that the effect of the system phase fluctuations on the measurement in PS-SS-OCT can be removed by using the proposed method. The method relies on a low-voltage broadband modulator, which can be driven by a synchronously triggered tone burst waveform from an arbitrary-waveform generator and the removal of the global phase offset of the measured Jones matrices by use of matrix normalization in postprocessing. The modulator driving scheme could work at a higher A-scan rate (> 10 kHz) on the ability of the generator used to generate a triggered tone burst waveform. The proposed method has the advantage over the direct-calibration method in extracting the locations of the sample surface since it does not require extracting the sample surface Jones matrix for each A-scan. This could be beneficial in situations where the surface Fresnel reflection is weak, e.g., when the surface is inclined relative to the beam or when matching liquids are used.

In summary, the method combines several advantages of previous PS-OCT systems. Continuous source modulation using sinusoidal drive waveforms multiplexes the polarization information in the depth direction rather than the lateral direction, thus improving lateral resolution, and low-voltage drive waveforms simplify the instrumentation significantly and aids clinic development. Low-voltage synchronous driving and software-based phase-offset removal provide optimum accuracy in the final retardance and orientation images with no additional calibration optics being required.

Acknowledgments

The authors acknowledge the contributions of M. Yamanari and Y. Yasuno from Tsukuba University in developing the system. This research was supported by EPSRC Grant No. EP/F020422.

References

1. J. F. deBoer, T. E. Milner, M. J. C. vanGemert, and J. S. Nelson, "Two-dimensional birefringence imaging in biological tissue by polarization-sensitive optical coherence tomography," *Opt. Lett.* **22**(12), 934–936 (1997).
2. M. Yamanari, S. Makita, and Y. Yasuno, "Polarization-sensitive swept-source optical coherence tomography with continuous source polarization modulation," *Opt. Express* **16**(8), 5892–5906 (2008).
3. B. H. Park, M. C. Pierce, B. Cense, and J. F. de Boer, "Jones matrix analysis for a polarization-sensitive optical coherence tomography system using fiber-optic components," *Opt. Letters* **29**(21), 2512–2514 (2004).
4. M. Yamanari, Y. Lim, S. Makita, and Y. Yasuno, "Visualization of phase retardation of deep posterior eye by polarization-sensitive swept-source optical coherence tomography with 1- μ m probe," *Opt. Express* **17**(15), 12385–12396 (2009).
5. Z. Lu, D. K. Kasaragod, and S. J. Matcher, "Optic axis determination by fibre-based polarization-sensitive swept-source optical coherence tomography," *Phys. Med. Biol.* **56**, 1–18 (2011).